Direct femtosecond laser inscription of Bragg gratings in Ho^{3+}/Pr^{3+} co-doped AlF_3-based glass fiber for 2.86 μm laser

NIANNIAN XU,[1] ZHIYONG YANG,[2] JIQUAN ZHANG,[1] NIAN LV,[1] MO LIU,[1] RUONING WANG,[1] ZHENRUI LI,[1] SHIJIE JIA,[1] GILBERTO BRAMBILLA,[3] SHUNBIN WANG,[1,5] AND PENGFEI WANG[1,4,6]

[1]*Key Laboratory of In-fiber Integrated Optics, Ministry Education of China, Harbin Engineering University, Harbin 150001, China*
[2]*Jiangsu Key Laboratory of Advanced Laser Materials and Devices, School of Physics and Electronic Engineering, Jiangsu Normal University, Xuzhou, Jiangsu 221116, China*
[3]*Optoelectronics Research Centre, University of Southampton, Southampton SO17 1BJ, UK*
[4]*Key Laboratory of Optoelectronic Devices and Systems of Ministry of Education and Guangdong Province, College of Optoelectronic Engineering, Shenzhen University, Shenzhen 518060, China*
[5]*e-mail: shunbinwang@hrbeu.edu.cn*
[6]*e-mail: pengfei.wang@tudublin.ie*

Received XX Month XXXX; revised XX Month, XXXX; accepted XX Month XXXX; posted XX Month XXXX (Doc. ID XXXXX); published XX Month XXXX

In this letter, we report the fabrication of fiber Bragg gratings (FBGs) in home-made Ho^{3+}/Pr^{3+} co-doped single-cladding fluoroaluminate (AlF_3) glass fibers and its application for Watt-level lasing at the mid-infrared (MIR) wavelength of 2.86 μm. The FBGs were inscribed using an 800 nm femtosecond (fs) laser direct-writing technique. The FBG properties were investigated for different pulse energies, inscription speeds, grating orders and transversal length. A 2nd-order FBG with a high reflectivity of 99% was obtained at one end of a 16.5 cm long gain fiber. Under 1150 nm laser pumping, this fiber yielded a power greater than 1 W at 2863.9 nm with an overall laser efficiency of 17.7%. The fiber laser showed a FWHM bandwidth of 0.46 nm and a long-term spectral stability.

http://dx.doi.org/10.1364/OL.99.09999

Fiber lasers have been widely investigated for their numerous applications in medical surgery, communication, sensing, material processing, molecule spectroscopy, defense and pump sources for other lasers [1-6]. Fluoride glasses based on ZrF_4, InF_3 and AlF_3 exhibit low phonon energy and wide spectral transmission range, and thus are excellent host materials for long wavelengths (λ) fiber lasers. In order to achieve high efficiency, dichroic mirrors (DM) with high reflectivity at the laser wavelength are widely used at the pump end of the fiber laser, increasing the complexity and instability of the laser system. Fiber Bragg gratings are passive devices which can be embedded into the fiber and provide an all-fiberized structure, which can effectively solve these problems. FBGs with small and uniform pitch (Λ ~0.5-3 μm), high reflectivity, good wavelength selectivity and narrow reflection linewidth, have attracted more and more attention in the last decade. So far, the writing of FBGs in fluoride fibers have mainly focused on fluorozirconate fibers. In 2007, Bernier *et al.* obtained a FBG with refractive index modulation of $\Delta n \sim 10^{-3}$ in Tm^{3+} -doped ZBLAN fibers [7], and also showed that the formation of grating was related to the negative refractive index change induced by femtosecond lasers. In 2018, Aydin *et al.* inscribed a 99.5% high reflectivity FBG and an 8% low reflectivity FBG in Er^{3+} -doped ZBLAN fiber, obtaining a laser output power of 41.6 W at 2.8 μm [8]: this is the highest laser output at ~3 μm, where FBGs played an important role in increasing the output power. The FBGs were written using a phase mask. While phase masks can only write gratings with a specific period or a small variation around it, the fs laser direct-writing technique allows to arbitrarily select the grating period (Λ), the Bragg wavelength (λ_B), the grating order (m), and its physical length (L), thus reflectivity (R) [9]. In 2017, Bharathan *et al.* wrote FBGs with R~0.5 in a Ho^{3+}/Pr^{3+} co-doped double-cladding ZBLAN fiber using line-by-line direct-writing method, and achieved a laser efficiency of 17% at λ ~2.88 μm [10]. In 2018, Goya *et al.* obtained an FBG with R~0.97 and $\Delta n \sim 1.1\times10^{-3}$ in Er^{3+}-doped ZBLAN fiber by plane-by-plane direct-writing technique, and obtained a laser efficiency of 29.1% at λ ~2.8 μm [11]. In 2019, Bharathan *et al.* wrote an FBG with a maximum coupling coefficient of κ ~464 m^{-1} using the stacking direct-writing method [12]. FBGs were also inscribed in fluoroindinate (InF_3) fibers: in 2020, Bharathan *et al.* wrote a grating with a high R at λ ~4 μm and κ ~275 m^{-1} after annealing at a temperature of T ~150 °C for 90 minutes [13]. Up to date, however, there has been no investigation of FBGs written in AlF_3 fiber for lasing. From the perspective of the glass matrix, AlF_3 glass has a higher glass transition temperature (~370 °C) and better corrosion resistance than ZBLAN and InF_3 glasses [14, 15]. Therefore, AlF_3 fiber FBGs are potentially useful for high power fiber lasers. In 2019, Wang *et al.* obtained a 10.4% laser output efficiency at λ ~2.9 μm by pumping a Ho^{3+}/Pr^{3+} co-doped AlF_3 fiber [16]. In 2021, Liu *et al.* obtained a room-temperature 1.13 W output power at λ ~2.9 μm in a Ho^{3+}/Pr^{3+} co-doped AlF_3 fiber [17]. By replacing DM with FBGs, the laser power and efficiency could be further improved.

Fs laser waveguide writing in various transparent materials requires little energy because of the multi-photon interactions [18-23], is not limited by the optical fiber photosensitivity, and provides extreme flexibility in terms of structure design. In this paper, FBGs with different parameters at λ_B ~2864 nm are successfully

inscribed into Ho^{3+}/Pr^{3+} co-doped AlF_3-based glass fibers using a fs laser with a line-by-line direct-writing method. A 17.7% efficiency continuous wave laser is obtained owing to a highly reflective Bragg grating (HR-FBG). The laser shows a stable laser wavelength and a long-term work stability.

Fig. 1 (a) shows a schematic setup of the fs laser direct-writing system used in this work. A Ti: Sapphire femtosecond laser system (*Solstice Ace*) emitted pulses at λ ~800 nm with a repetition rate of 1 kHz and a duration of 100 fs (full width half-maximum, FWHM). A beam splitter with ratio of 9:1 was placed after the fs laser to reduce the laser energy. The laser beam was then focused into the home-made AlF_3 fiber core using a 40× objective with a numerical aperture (NA) of ~0.65 (*Olympus*). To avoid aberrations at the curved air-glass interface, the AlF_3 fiber was immersed in refractive index matching oil and then covered with a 100 μm thick glass coverslip. The fiber was held straight by a customized, precisely-adjustable, three-dimensional translation stage (*X: XMS100-S; Y: XMS100-S; Z: VP-5ZA, XPS-D*). Each grating plane was inscribed by moving the fiber in relation to the focus of the laser beam for a distance of l (transversal length). As shown in Fig. 1 (b), each grating plane is separated by a distance Λ. The pulse train was blocked by a mechanical shutter during the movements represented by the dashed path. A mid-IR supercontinuum source was assembled and an optical spectrum analyzer (OSA, Yokogawa AQ6377) with a 200-pm resolution was used for the spectral characterization.

The AlF_3 fiber was fabricated by using the rod-in-tube method. The composition of the core was $30AlF_3$-$10BaF_2$-$19CaF_2$-$7.3YF_3$-$12.5SrF_2$-$2.5PbF_2$-$3.5MgF_2$-$3LiF$-$10ZrF_4$-$2HoF_3$-$0.2PrF_3$ (mol%). The fiber had a core diameter of 10.5 μm, a NA ~0.27 and a cladding diameter of 225 μm. The cut-off wavelength at λ ~3.69 μm effectively provided two modes at λ ~2864 nm. During the grating characterization experiments, the launched light beamoffset was minimized to achieve the maximum coupling into the fundamental mode. The background loss of the fiber at λ ~793 nm was estimated to be ~1.6 dB/m by using the cut-back method.

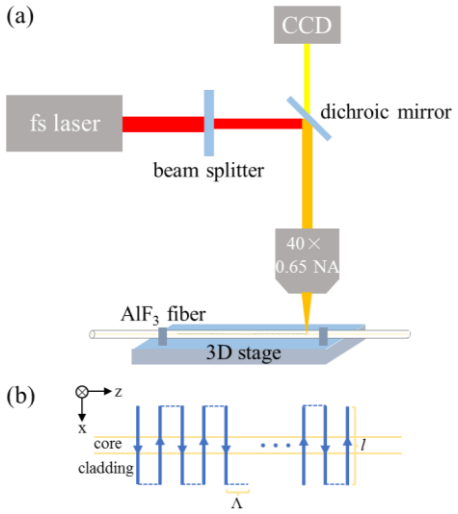

Fig. 1 (a). Schematic of fs laser fabricating FBGs system. (b). The pattern of FBGs processing path (top-view).

In order to estimate the optimal pulse energy (E_p) for FBG writing, a series of second order gratings with Λ ~1.92 μm, l ~30 μm, L ~8 mm and λ_B ~2864 nm were written with E_p ~2.4 μJ, 2.8 μJ, 3.2 μJ, respectively. The inscription speed of all the FBGs was 60 μm/s. The total inscription time of each FBG was approximately 1 h. Fig. 2 (a) and (b) show microscope images of the FBGs inscribed with E_p ~2.4 μJ and 3.2 μJ. The grating plane inscribed at E_p ~2.4 μJ exhibited a small visibility, while that at E_p ~3.2 μJ was clear. Fig. 2 (c), (d) show the top and side views at 2.8 μJ. The side view shows that the grating was written into the fiber core, leading to a certain depth. Fig. 2 (e) shows the FBGs transmission spectra at different pulse energies. At increasing E_p, the corresponding resonance dip increase from 11.9 dB to a maximum of 19.6 dB and then fell to 13.6 dB. The increase was attributed to the rising Δn caused by the gradual E_p increase, while the fall resulted from damage in the core, possibly due to the energy exceeding the damage threshold of the AlF_3 fiber. Correspondingly, the insertion losses introduced by the gratings increased for increasing E_p from 0.6 dB to 1 dB and 1.28 dB respectively. The side peak at λ ~2852 nm can be ascribed to cross-coupling between modes, i.e., fundamental mode to second-order modes or second-order modes to fundamental mode [24-26].

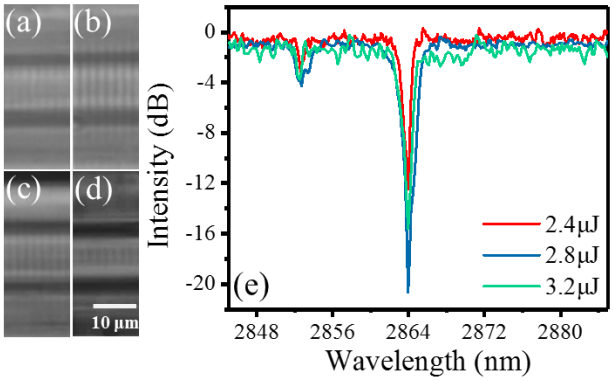

Fig. 2. Microscope images of FBGs inscribed with E_p of (a) 2.4 μJ (top view), (b) 3.2 μJ (top view) and (c, d) 2.8 μJ, (c: top view; d: side view). (e) Transmission spectra of the FBGs at different pulse energies.

The inscription speed is also an essential parameter for FBG writing: values of 30 μm/s, 60 μm/s and 120 μm/s were used for inscribing 2nd-order gratings with E_p ~2.8 μJ, Λ ~1.92 μm, l ~30 μm, and L~8 mm. As shown in Fig. 3 (a), a dip of 13.6 dB was achieved when FBGs was inscribed at 30 μm/s, smaller than that of 19.6 dB at 60 μm/s, but larger than that of 10.6 dB at 120 μm/s. Moreover, as the speed increased, the insertion losses of FBGs were 0.53 dB, 1 dB and 1.2 dB, respectively. Fig. 3 (b), (c) and (d) show microscope images of the transverse cross section at speeds of 30 μm/s, 60 μm/s and 120 μm/s (the red dashed line is the profile of the core): a smoother grating plane was written into core at lower speeds because of sufficient spatial overlap of pulses at 30 μm/s compared with the irregular grating structure at 120 μm/s. The speed of 60 μm/s was chosen as an overall balance, considering also the FBG uniformity and resonance strength.

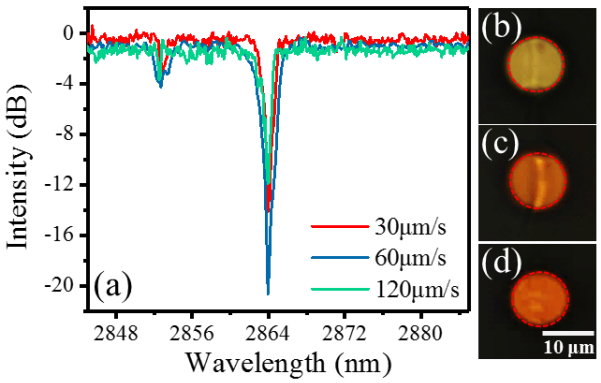

Fig. 3 (a). Transmission spectra of the FBGs at different inscription speeds. (b-d). Transverse cross section of the modification in AlF_3 fiber with different inscription speeds.

FBGs of different m orders were investigated. All the FBGs were written with E_p ~2.8 μJ, speed of 60 μm/s, l ~30 μm and L ~8 mm, while the grating pitch was changed from Λ ~1.92 μm to 2.88 μm and 3.84 μm, for m =2, 3, and 4, respectively, corresponding to the central wavelength of λ_B ~2.86 μm. The first-order grating was difficult to inscribe probably due to the overlap of adjacent grating planes. Fig. 4 (a) suggests that the biggest resonance dip of 19.6 dB was obtained for m =2. The strengths for m =3 and 4 were 16.9 dB and 13.4 dB, respectively. As increasing m, the Bragg resonance of the FBG gradually decreases. The reason could be that for higher-order gratings, nonsinusoidal refractive index perturbation is formed, which is related to the expansion of Fourier series. And the order of the Fourier series and perturbation are negatively correlated [27,28]. Thus, the2nd-order gratings caused the strongest perturbation, and biggest resonance strength. Besides, 2nd-order gratings of different transversal lengths (l) were discussed in AlF_3-based fiber. The grating with l ~20 μm showed a dip of 17 dB, which was smaller than that of 19.6 dB observed at l ~30 μm (see Fig. 4 (b)). The result involved a slightly smaller modulation depth along the y-axis and shallower modulation traces when the transversal length was shorter.

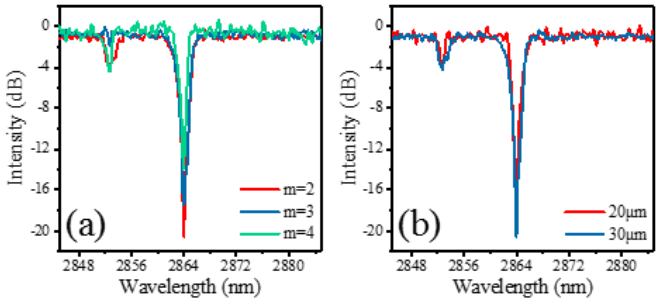

Fig. 4 (a). Transmission spectra of the FBGs with different orders m. (b). FBG transmission spectra for different transversal length l.

Fig. 5 shows a schematic of experimental setup used for 2.86 μm laser testing. A λ ~1150 nm Raman fiber laser was used as pump source and launched through a commercial HI1060 standard fiber with a fiber collimator at the end. L3 had a focal length of 6 mm. A length of 16.5 cm Ho^{3+}/Pr^{3+} co-doped AlF_3-based glass fiber was selected as the gain medium of the laser cavity. The laser cavity mirrors were formed by inscribing a high reflectivity grating (HR-FBG, R≈99%) into the fiber at one extremity and exploiting Fresnel reflection (~4% at 2.86 μm) at the other extremity. Most of the fiber was placed on a copper plate with active cooling to reduce heat load. A 2 m long InF_3-based fiber cable (Thorlabs MF21L2) with a core diameter of 200 μm and NA ~0.26 was connected to the OSA (AQ6377) to detect the output laser spectra. A power meter (Thorlabs PM100D) was used to measure the output power value.

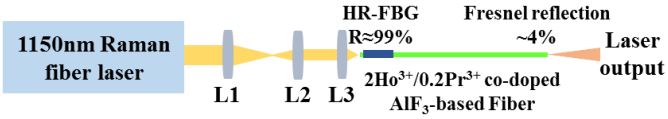

Fig. 5. Schematic diagram for the fiber laser experiments at λ ~2.86 μm.

Fig. 6 showed the dependence of the output power at λ ~2864 nm with respect to the absorbed pump power at λ ~1150 nm. As the absorbed pump power increased to 30.67 mW, lasing at 2863.9 nm was observed. A maximum output power of 1006 mW (with no 1150 nm residual pump power) was achieved when the absorbed pump power was increased to 5.7 W. The linear fit provided a slope efficiency of 17.7%. Fig. 7 shows the output laser spectra as a function of wavelength at output powers of 5 mW, 367 mW, 604 mW and 977 mW. The center wavelength remained constant under different output powers. While at low power the central wavelength was 2863.9 nm, at 977 mW, it shifted to 2863.88 nm, within the spectrometer measurement error range. The inset shows the laser spectrum in the wavelength range of 2820 nm – 2910 nm at an output power of 977 mW: the laser line FWHM was 0.46 nm.

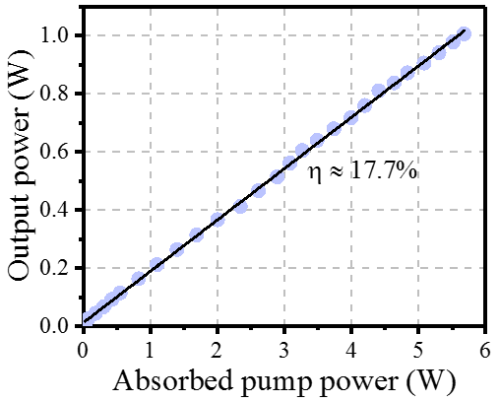

Fig. 6. Laser output power at 2.86 μm as a function of the absorbed pump power at 1150 nm.

The stability of output power was also tested over a period of 30 minutes, as shown in Fig. 8. The RMS fluctuation for the output power is 0.52%. As the gain fiber at the pump side was not fully protected by the heat sink, the thermal expansion of fiber with a ~10.5 μm core caused a change in the focus position of the pump beam, thus the value of the output power presented a decreasing trend.

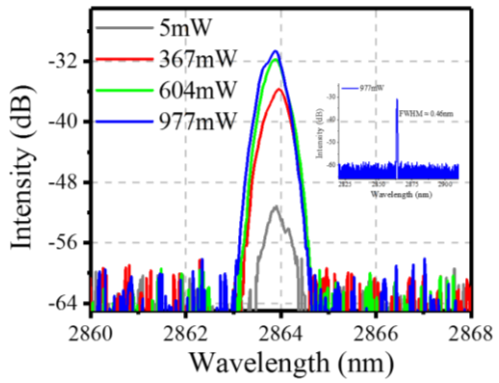

Fig. 7. Laser spectra at output powers of 5, 367, 604 and 977 mW (inset: laser spectrum at the output power of 977 mW).

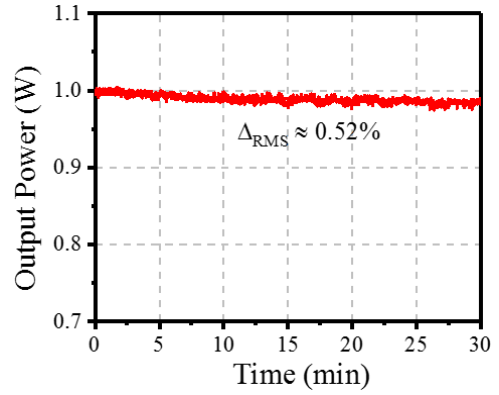

Fig. 8. Output power temporal stability.

In conclusion, FBGs with different parameters were first successfully written into AlF_3-based fibers at the MIR wavelength of λ ~2.86 μm. The best FBG writing conditions were achieved for pulse energy of and speed of 2.8 μJ and 60 μm/s, respectively. A 2nd-order FBG with 30 μm transversal length showed a strong dip, and was exploited to inscribe a high reflectivity mirror for the laser cavity. A 16.5 cm long stretch of Ho^{3+}/Pr^{3+} co-doped single-cladding AlF_3-based fiber was used as lasing medium and produced a maximum output power of 1006 mW with an overall slope efficiency of 17.7%.

Funding. This work was supported by the National Natural Science Foundation of China (NSFC) under Grant No. of 61935006, 62090062, 62005060, 61905048, 62005061 and Heilongjiang Provincial Natural Science Foundation of China (LH2020F030), National Key R&D Program of China under Grant No. of 2020YFA0607602 and the Shenzhen Basic Research Project under Grant No. of JCYJ20190808173619062. The 111 project (B13015) to the Harbin Engineering University and Heilongjiang Touyan Innovation Team Program. The Fundamental Research Funds for the Central Universities (3072021CF2514，3072021CF2533).

Disclosures. The authors declare no conflicts of interest.

Data availability. Data underlying the results presented in this paper are not publicly available at this time but may be obtained from the authors upon reasonable request.

References

1. M. Pollnau. IEEE Journal of Quantum Electronics **39**, 350 (2003).
2. M. Pollnau and S. D. Jackson, IEEE Journal of Quantum Electronics **38**, 162 (2002).
3. X. Zhu and R. Jain. Opt. Lett. **32**, 2381 (2007).
4. S. Tokita, M. Murakami, S. Shimizu, M. Hashida, and S. Sakabe. Opt. Lett. **36**, 2812 (2011).
5. S. Tokita, M. Hirokane, M. Murakami, S. Shimizu, M. Hashida, and S. Sakabe. Opt. Lett. **35**, 3943 (2010).
6. I. Kubat, C. R. Petersen, U. V. Møller, A. Seddon, T. Benson, L. Brilland, D. Méchin, P. M. Moselund, and Ole Bang. Opt. Express **22**, 3959 (2014).
7. M. Bernier, D. Faucher, R. Vallée, A. Saliminia, G. Androz, Y. Sheng, and S. L. Chin. Opt. Lett. **32**, 454 (2007).
8. Y. O. Aydin, V. Fortin, R. Vallée, and M. Bernier. Opt. Lett. **43**, 4542.(2018).
9. E. Ertorer, M. Haque, J. Li, and P. R. Herman. Opt. Express **26**, 9323 (2018).
10. G.Bharathan, R. I. Woodward, M. Ams, D. D. Hudson, S. D. Jackson, and A. Fuerbach. Opt Express **25**, 30013-30019 (2017).
11. K. Goya, H. Matsukuma, H. Uehara, S. Hattori, C. Schäfer, D. Konishi, M. Murakami, and S. Tokita. Opt. Express **26**, 33305 (2018).
12. G. Bharathan, T. T. Fernandez, M. Ams, R. I. Woodward, D. D. Hudson, and A. Fuerbach. Opt. Lett. **44**, 423-426 (2019).
13. G. Bharathan, T. T. Fernandez, M. Ams. Opt. Lett. **45**, 4316 (2020).
14. J.Bei et al. Opt. Mater. Express **4**, 1213 (2014).
15. F. G. Heinz, H. Bruno. J Non-Cryst Solids **284**, 105 (2001).
16. S. Wang, J. Zhang, N. Xu, S. Jia, G. Brambilla, and P. Wang. Opt. Lett. **45**, 1216 (2020).
17. M. Liu. J. Zhang, N. Xu, X. Tian, S. Jia, S. Wang, G. Brambilla, and P.Wang. Opt. Lett. **46**, 2417 (2021).
18. A. Theodosiou, A. Lacraz, A. Stassis, C. Koutsides, M. Komodromos, K. Kalli. J. Lightwave Technol **35**, 5404-5410 (2017).
19. Z. Liu, Y. Liao, Z. Fang, W. Chu, Y. Cheng,. Sci. China Phys. Mech. Astron **61**, 70322 (2018).
20. A. Drouin, P. Lorre, J. Boisvert, S. Loranger, V. L. Iezzi, and R. Kashyap. Opt. Express **27**, 2488 (2019).
21. G. Roth, S. Hessler, S. Kefer, M. Girschikofsky, C. Esen, and R.Hellmann. Opt. Express **28**, 18077 (2020).
22. G.R. Castillo-Vega, E. H. Penilla, S. Camacho-López, G. Aguilar, and J. E. Garay. Opt. Mater. Express **2**, 1416 (2012).
23. J. Lapointe, J. Bérubé, Y. Ledemi, A. Dupont, V. Fortin, Y. Messaddeq, R.Vallée. Light Sci Appl **9**, 64 (2020).
24. B. Sun, A. Wang, L. Xu, C. Gu, Z. Lin, H. Ming, Q. Zhan. Opt. Lett. 37, 464-466 (2012).
25. Wu, C., Liu, Z., Chung, K. M., Tse, M. L. V., Chan, F. Y. M., Lau, A. P. T. IEEE Photonics Journal 4, 1080-1086 (2012).
26. Huang, T., Fu, S., Ke, C., Shum, P. P., & Liu, D. IEEE Photonics Technology Letters 26, 1908-1911 (2014).
27. M. Ams, P. Dekker, S. Gross, J. M. Withford. Nanophotonics. 6(5), 743-763 (2017).
28. G. D. Marshall, R. J. Williams, N. Jovanovic, M. J. Steel, M. J. Withford. Opt. Express 18, 19844 (2010).

Full citation listings

[1] Markus Pollnau, Analysis of heat generation and thermal lensing in erbium 3 μm lasers. IEEE Journal of Quantum Electronics 39, 350-357 (2003).

[2] Markus Pollnau and Stuart D. Jackson, Energy recycling versus lifetime quenching in erbium-doped 3 μm fiber lasers. IEEE Journal of Quantum Electronics 38, 162-169 (2002).

[3] Xiushan Zhu and Ravi Jain, Compact 2 W wavelength-tunable Er: ZBLAN mid-infrared fiber laser. Opt. Lett. 32, 2381-2383 (2007).

[4] Shigeki Tokita, Masanao Murakami, Seiji Shimizu, Masaki Hashida, and Shuji Sakabe, 12 W Q-switched Er: ZBLAN fiber laser at 2.8 μm. Opt. Lett. 36, 2812-2814 (2011).

[5] Shigeki Tokita, Mayu Hirokane, Masanao Murakami, Seiji Shimizu, Masaki Hashida, and Shuji Sakabe, Stable 10 W Er: ZBLAN fiber laser operating at 2.71–2.88 μm. Opt. Lett. 35, 3943-3945 (2010).

[6] Irnis Kubat, Christian Rosenberg Petersen, Uffe Visbech Møller, Angela Seddon, Trevor Benson, Laurent Brilland, David Méchin, Peter M. Moselund, and Ole Bang, Thulium pumped mid-infrared 0.9–9 μm supercontinuum generation in concatenated fluoride and chalcogenide glass fibers. Opt. Express 22, 3959-3967 (2014).

[7] M. Bernier, D. Faucher, R. Vallée, A. Saliminia, G. Androz, Y. Sheng, and S. L. Chin, Bragg gratings photoinduced in ZBLAN fibers by femtosecond pulses at 800 nm. Opt. Lett. 32, 454-456 (2007).

[8] Yigit Ozan Aydin, Vincent Fortin, Réal Vallée, and Martin Bernier, Towards power scaling of 2.8 μm fiber lasers. Opt. Lett. 43, 4542-4545 (2018).

[9] Erden Ertorer, Moez Haque, Jianzhao Li, and Peter R. Herman, Femtosecond laser filaments for rapid and flexible writing of fiber Bragg grating. Opt. Express 26, 9323-9331 (2018).

[10] Gayathri Bharathan, Robert I. Woodward, Martin Ams, Darren D. Hudson, Stuart D. Jackson, and Alex Fuerbach, Direct inscription of Bragg gratings into coated fluoride fibers for widely tunable and robust mid-infrared lasers. Opt Express 25, 30013-30019 (2017).

[11] Kenji Goya, Hiraku Matsukuma, Hiyori Uehara, Satoshi Hattori, Christian Schäfer, Daisuke Konishi, Masanao Murakami, and Shigeki Tokita, Plane-by-plane femtosecond laser inscription of first-order fiber Bragg gratings in fluoride glass fiber for in situ monitoring of lasing evolution. Opt. Express 26, 33305-33313 (2018).

[12] Gayathri Bharathan, Toney Teddy Fernandez, Martin Ams, Robert I. Woodward, Darren D. Hudson, and Alex Fuerbach, Optimized laser-written ZBLAN fiber Bragg gratings with high reflectivity and low loss. Opt. Lett. 44, 423-426 (2019).

[13] Gayathri Bharathan, Toney Teddy Fernandez, Martin Ams, Jean-Yves Carrée, Samuel Poulain, Marcel Poulain, and Alex Fuerbach, Femtosecond laser direct-written fiber Bragg gratings with high reflectivity and low loss at wavelengths beyond 4 μm. Opt. Lett. 45, 4316-4319 (2020).

[14] Jiafang Bei, Herbert Tze Cheung Foo, Gujie Qian, Tanya M. Monro, Alexander Hemming, and Heike Ebendorff-Heidepriem, Experimental study of chemical durability of fluorozirconate and fluoroindate glasses in deionized water. Opt. Mater. Express 4, 1213-1226 (2014).

[15] Frischat Guenther Heinz, Hueber Bruno, Chemical stability of ZrF_4- and AlF_3-based heavy metal fluoride glasses in water. J Non-Cryst Solids 284, 105-109 (2001).

[16] Shunbin Wang, Jiquan Zhang, Niannian Xu, Shijie Jia, Gilberto Brambilla, and Pengfei Wang, 2.9 μm lasing from a Ho^{3+}/Pr^{3+} co-doped AlF_3-based glass fiber pumped by a 1150 nm laser. Opt. Lett. 45, 1216-1219 (2020).

[17] Mo Liu, Jiquan Zhang, Niannian Xu, Xinwei Tian, Shijie Jia, Shunbin Wang, Gilberto Brambilla, and Pengfei Wang, Room-temperature watt-level and tunable ~3 μm lasers in Ho^{3+}/Pr^{3+} co-doped AlF_3-based glass fiber. Opt. Lett. 46, 2417-2420 (2021).

[18] AntreasTheodosiou, Amedee Lacraz, Andreas Stassis, Charalambos Koutsides, Michael Komodromos, Kyriacos Kalli, Plane-by-Plane Femtosecond Laser Inscription Method for Single-Peak Bragg Gratings in Multimode CYTOP Polymer Optical Fiber. J. Lightwave Technol 35, 5404-5410 (2017).

[19] Zhengming Liu, Yang Liao, Zhiwei Fang, Wei Chu, Ya Cheng, Suppression of bend loss in writing of three-dimensional optical waveguides with femtosecond laser pulses. Sci. China Phys. Mech. Astron 61, 70322 (2018).

[20] Antoine Drouin, Pierre Lorre, Jean-Sébastien Boisvert, Sébastien Loranger, Victor Lambin Iezzi, and Raman Kashyap, Spatially resolved cross-sectional refractive index profile of fs laser–written waveguides using a genetic algorithm. Opt. Express 27, 2488-2498 (2019).

[21] Gian-Luca Roth, Steffen Hessler, Stefan Kefer, Maiko Girschikofsky, Cemal Esen, and Ralf Hellmann, Femtosecond laser inscription of waveguides and Bragg gratings in transparent cyclic olefin copolymers. Opt. Express 28, 18077-18084 (2020).

[22] Gabriel R. Castillo-Vega, Elías H. Penilla, Santiago Camacho-López, Guillermo Aguilar, and J. E. Garay, Waveguide-like structures written in transparent polycrystalline ceramics with an ultra-low fluence femtosecond laser. Opt. Mater. Express 2, 1416-1424 (2012).

[23] Jerome Lapointe, Jean-Philippe Bérubé, Yannick Ledemi, Albert Dupont, Vincent Fortin, Younes Messaddeq, Réal Vallée, Nonlinear increase, invisibility, and sign inversion of a localized fs-laser-induced refractive index change in crystals and glasses. Light Sci Appl 9, 64 (2020).

[24] Biao Sun, Anting Wang, Lixin Xu, Chun Gu, Zhongxi Lin, Hai Ming, Qiwen Zhan, Low-threshold single-wavelength all-fiber laser generating cylindrical vector beams using a few-mode fiber Bragg grating. Opt. Lett. 37, 464-466 (2012).

[25] Chuang Wu, Zhengyong Liu, Kit Man Chung, Ming-Leung Vincent Tse, Florence Y. M. Chan, Alan Pak Tao Lau, Chao Lu, Haw-Yaw Tam, Strong LP_{01} and LP_{11} mutual coupling conversion in a two-mode fiber Bragg grating. IEEE Photonics Journal. 4, 1080-1086 (2012).

[26] Huang, T., Fu, S., Ke, C., Shum, P. P., & Liu, D, Characterization of fiber Bragg grating inscribed in few-mode silica-germanate fiber. IEEE Photonics Technology Letters 26, 1908-1911 (2014)

[27] Ams. M, Dekker P, Gross. S, Withford. M. J, Fabricating waveguide bragg gratings (WBGs) in bulk materials using ultrashort laser pulses. Nanophotonics. 6(5), 743-763 (2017).

[28] Marshall Graham D, Williams Robert J, Jovanovic Nemanja, Steel M. J, Withford Michael J, Point-by-point written fiber Bragg gratings and their application in complex grating designs. Opt. Express 18, 19844-19859 (2010).